Available online at www.sciencedirect.com
SCIENCE DIRECT®
Pergamon
Acta Materialia 51 (2003) 5051–5062
Acta MATERIALIA
www.actamat-journals.com

Hybrid modelling of aluminium–magnesium alloys during thermomechanical processing in terms of physically-based, neuro-fuzzy and finite element models

Q. Zhu [a,*], M.F. Abbod [b], J. Talamantes-Silva [c], C.M. Sellars [a], D.A. Linkens [b], J.H. Beynon [a]

[a] *Department of Engineering Materials, The University of Sheffield, Mappin Street, Sheffield S1 3JD, UK*
[b] *Department of Automatic Control and System Engineering, The University of Sheffield, Mappin Street, Sheffield S1 3JD, UK*
[c] *Department of Mechanical Engineering, The University of Sheffield, Mappin Street, Sheffield S1 3JD, UK*

Received 15 August 2002; accepted 9 June 2003

Abstract

For modern metals industries using thermomechanical processing, off-line modelling and on-line control based on physical knowledge are highly desirable in order to improve the quality of existing materials, the time and cost efficiency, and to develop new materials. Neural network and neuro-fuzzy models are the most popular tools, but they do not embed physical knowledge. On the other hand, current physically-based models are too complex for industrial application and are less efficient than neural networks. A combination of neuro-fuzzy and physically-based models has therefore been developed, which is termed a "hybrid model". The hybrid model has been applied to predict flow stress and microstructural evolution during thermomechanical processing. Comparison with experimental data shows generally good agreement for Al–1% Mg alloy deformed under thermomechanical processing conditions. The hybrid model was then embedded into a finite element model and the simulated results show a very similar distribution to those calculated using empirical models.

Keywords: Physically-based modelling; Neuro-fuzzy modelling; Finite element modelling; Microstructure; Thermomechanical processing; Aluminium alloys

1. Introduction

Modelling is now an integral part of the strategies for developing more efficient materials processing practice, for achieving tighter specifications, for improving mechanical properties, particularly on small batches, and for providing customers with the high quality products they require. There is a wide range of modelling techniques employed and these are under continual development (e.g. Refs. [1,2]). The techniques range from detailed off-line models to simple algorithms for on-line control of thermomechanical processing. For off-line modelling, physically-

* Corresponding author. Tel.: +44-114-222-7749.
E-mail address: q.zhu@sheffield.ac.uk (Q. Zhu).

1359-6454/$30.00
doi:10.1016/S1359-6454(03)00353-7

based models (or so-called white-box models) have the most significant potential in the future in terms of providing the best understanding of the physical processes, while for on-line control, neural network models (or so-called black-box models) are the most computationally efficient tools.

Most physically-based models for plastic deformation behaviour utilise the internal state variables such as the internal dislocation density, the spacing between dislocation subboundaries and the misorientation across the subboundaries [3–10]. The internal state variables are the main factors which control flow stress and dynamic or subsequent static recrystallisation behaviour. The evolution of the internal state variables during plastic deformation is in turn dominated by the type of material being worked, the composition of the material and the deformation conditions, such as temperature, strain rate and time. Previous results [8–10] show that for modelling microstructural evolution under changing deformation conditions in plane strain compression (PSC) testing (e.g. under conditions of transient strain rate), which is close to industrial thermomechanical processing conditions, the kinetic laws for internal state variables must be in differential form and the geometrically necessary dislocations must be taken into account. By using the above mentioned concepts, the evolution of internal state variables and subsequent recrystallisation behaviour can be described quantitatively [9,10].

Neural network or neuro-fuzzy models work efficiently and can be used for on-line control. The main limitation of these models is that they work in an opaque manner (black-box). In order to transform the black-box from "opaque" to "translucent", physical knowledge about the process being modelled should be incorporated into the black-box. The combination of physically-based and black-box models, which is termed a "hybrid model" and used in the present paper, is an attractive way to develop translucent models for better modelling of thermomechanical processing. Hybrid modelling techniques therefore provide good modelling tools that combine different modelling approaches in a single dynamic model [11]. While the physically-based models ensure that the results are physically sensible, the black-box models can be utilised to increase the accuracy of fitting the experimental results. Initial modelling results show that the hybrid model is a successful tool for modelling flow stress and evolution of microstructures during thermomechanical processing [12–14].

The finite element modelling (FEM) technique has become popular in recent years for simulating metal forming processes. For FEM, the relationships between inputs and outputs are needed [15]. In traditional FEM of thermomechanical processing of metals, these relationships are based on empirical equations, which are derived from experimental results. Such relationships for flow stress, recrystallisation kinetics and recrystallised grain size in terms of the applied strain, strain rate and temperature in deformation passes and the time–temperature history between passes have been widely applied to model the microstructural evolution of steels during industrial hot rolling [16]. These empirical microstructural equations are, however, less successful for aluminium alloys and for steels when the local changing conditions of strain rate and temperature and strain path are considered [17]. These empirical equations also have limitations, as they are difficult to extrapolate to other materials or processing conditions. Therefore, it is highly desirable to have more powerful and physically-based tools to relate the input parameters and output properties such as microstructures and materials properties. The hybrid modelling technique mentioned above is potentially such a tool and is embedded within a finite element code. The FEM results calculated using empirical equations and the developed hybrid models are compared with each other in the present paper.

2. Basics of hybrid models

2.1. Physically-based models

The physically-based models used in the present paper have been described in detail elsewhere [7–10]. The physically-based equations are summarised below.

The internal dislocation density ρ_i consists of two parts, i.e. the so-called "random" dislocation density ρ_r and the "geometrically necessary" dislo-

cation density ρ_g, i.e. $\rho_i = \rho_r + \rho_g$. The values of ρ_r and ρ_g can be obtained using the following equations [8,9], respectively

$$\rho_r = \int_0^{\varepsilon} d\rho_r^+ + d\rho_r^- = \int_0^{\varepsilon} \left(C_1 - C_2 \frac{\sigma_f}{Z} \rho_r \right) d\varepsilon \quad (1)$$

$$\rho_g = \frac{1}{b} \left(\frac{1}{\bar{R}} - \frac{\theta}{\delta} \right) \quad (2)$$

where C_1 and C_2 are material constants, b is the Burgers vector, $1/\bar{R}$ is the local lattice curvature within a grain and σ_f is the friction stress arising from the interaction of dislocation glide and solute atoms, which depends on the Zener Hollomon parameter $Z = \dot{\varepsilon}\exp(Q/RT)$, where $\dot{\varepsilon}$ is strain rate, Q is the activation energy for deformation, T is the absolute temperature and R is the gas constant.

The evolution of spacing between subboundaries, i.e. subgrain size δ and misorientation angle across the subboundaries θ can be written as,

$$\delta = \int_0^{\varepsilon} \frac{\delta}{\varepsilon_\delta \delta_{ss}} (\delta_{ss} - \delta) d\varepsilon \quad (3)$$

$$\theta = \int_0^{\varepsilon} \frac{1}{\varepsilon_\theta} (\theta_{ss} - \theta) d\varepsilon \quad (4)$$

where ε_δ and ε_θ are characteristic strains relating to deformation conditions, and the subscript ss means steady state.

Flow stress σ can be written by

$$\sigma = \sigma_{\rho_i} + \sigma_\delta + \sigma_f + \sigma_d + \sigma_p \quad (5)$$

$$\sigma_{\rho_i} = \alpha_1 MGb\rho_i^{1/2} \quad (6)$$

$$\sigma_\delta = \alpha_2 MGb/\delta \quad (7)$$

where α_1 and α_2 are materials constants, σ_d and σ_p are the stresses arising from the grain boundaries and second phase particles, which can be assumed to be negligible for the experimental alloys which have single phase and grain size significantly larger than subgrain size, M is the Taylor factor and G is the shear modulus.

Nucleation of recrystallisation at grain boundary surfaces is the dominant term for a large regime of deformation. This strain regime covers most thermomechanical processing conditions and the following simplified equation of nucleation density N_V [9] is used

$$N_V = p_3 \lambda_3 \frac{S_V}{\delta^2} \quad (8)$$

where p_3 is the probability of finding subgrains with a size larger than a critical value that can provide the nuclei for recrystallisation, λ_3 is a geometric parameter and S_V is the grain boundary surface area per unit volume, which increases with strain.

For site-saturation, recrystallisation kinetics is determined by both nucleation density and the mean growth rate $\bar{G}$ of the nuclei for recrystallisation fractions between 0 and 0.5, by [9]

$$t_{50} = C_3 \bar{G}^{-1} N_V^{-1/3} \quad (9)$$

$$\bar{G} = M_{gb} P_D \quad (10)$$

where C_3 is a geometrical constant, M_{gb} is the grain boundary mobility and P_D is the total stored energy per unit volume, which can be calculated by [9]

$$P_D = \frac{Gb^2}{10} \left[\rho_i (1 - \ln(10b\rho_i^{1/2})) + \frac{2\theta}{b\delta} \left(1 + \ln\left(\frac{\theta_c}{\theta} \right) \right) \right] \quad (11)$$

where θ_c is the critical angle for distinguishing between a grain boundary and a subgrain boundary, and is assumed to be 15° in this paper.

For site-saturated nucleation, grain size is simply calculated from nucleation density by [9]

$$d_{rex} = A N_V^{-1/3} \quad (12)$$

where A is a geometric parameter ($A = 2.347$ for a grain structure of uniform tetrakaidecahedra).

2.2. Basics of black-box models

Neuro-fuzzy models provide a good tool for modelling the material properties as they provide capabilities of interpolation and combination with different models for various alloys within a single model that can describe the material behaviour under different deformation conditions [12–14]. One particular neuro-fuzzy model structure, which is used in this research, is the Takagi–Sugeno–Kang auto regressive model (TSK-ARM) [18]. The model is based on linguistic antecedents and parametric consequent rules and trained using recursive techniques. The syntax of the fuzzy rules has fuzzy

sets in the antecedent part and a regression model as the consequence in the following form

$$\text{If } x_1 \text{ is } B^1 \text{ and } \ldots \text{ and } x_n \text{ is } B^n \text{ then } y = c_0 + c_1x_1 + \ldots + c_nx_n \quad (13)$$

where $x = (x_1,\ldots,x_n)^T$ and y are the input and output linguistic variables, while B^i and c_i are the linguistic values characterised using membership functions. The form of the rule representation gives more information and thus the number of rules required is much less than for traditional relational fuzzy models [19]. In the model, a complex high dimensional problem with non-linear modelling is decomposed into a set of simple linear models that are valid within certain operating regions defined by fuzzy boundaries. The fuzzy interface is then used to interpolate the outputs of the local models in a smooth fashion to obtain a global model. As a result, the approach provides a better modelling accuracy than equivalent relational fuzzy models.

A single input–single output system can be modelled by the method described in Ref. [18]. It is reasonable to assume that the input space can be spanned by fuzzy partitions and that the system can be represented by fuzzy implications, i.e. by one rule in each fuzzy sub-space, and thus the model can be rewritten as

L^i: if $y(t)$ is B' then

$$\Delta y_m(t+1) = \Theta'\Phi(t) \quad (14)$$

$$\Phi(t) = [-\Delta y(t), -\Delta y(t-1),\ldots,-\Delta y(t-n_a+1), \Delta u(t), \Delta u(t-1),\ldots, \Delta u(t-n_b+1)]^T \quad (15)$$

and Θ' represents a vector of the β_i-weighted parameters of Θ, such that:

$$\Theta' = [a'_1, a'_2 \ldots a'_{n_a}, b'_1, b'_2 \ldots b'_{n_b}] \quad (16)$$

$$a'_i = \sum_{j=1}^{p} \beta_j a_i^j \qquad i = 1,\ldots,n_a \quad (17)$$

$$b'_k = \sum_{j=1}^{p} \beta_j b_k^j \qquad k = 1,\ldots, n_b \quad (18)$$

$$\beta_i = \frac{B^i[y(t)]}{\sum_{i=1}^{p} B^i[y(t)]} \quad (19)$$

where a'_i and b'_k are the polynomials of the TSK equation, $\Delta y_m(t+1)$ in Eq. (14) is the one-step-ahead model prediction at t, $\Delta y(t)$ and $\Delta u(t)$ in Eq. (15) are the process inputs and outputs at time t.

3. Methodology of the hybrid model

The hybrid modelling is carried out by combining the developed physically-based models and the neuro-fuzzy TSK-ARM models, as shown in Fig. 1. In the hybrid modelling, the inputs are the deformation conditions such as strain rate $\dot{\varepsilon}$, temperature T and strain ε for a given material. Fig. 2 shows a schematic diagram of the modules used in the modelling of thermomechanical processing. The friction stress is at present difficult to calculate theoretically and hence is calculated using the neuro-fuzzy model which is trained on the experimental results [8]. The internal state variables such as internal dislocation density (ρ_i), spacing between subboundaries (δ) and misorientation across the subboundaries (θ) are calculated by both physically-based models and neuro-fuzzy models using the principle of hybrid modelling. The internal state variables calculated by both component models are then combined to provide a new set of data. These variables are then used as inputs for further calculation of stress components σ_{ρ_i}, σ_δ, P_D, N_V and $\bar{G}$ using physically-based models. The flow stress σ, the time of 50% recrystallisation t_{50} and recrystallised grain size d_{rex} are then finally calculated. During the calculation of flow stress, any misfit is compensated using the model that calculates the friction stress. The details of the training process some validations of the hybrid modelling can be found elsewhere [12–14].

4. Application of the hybrid model to finite element modelling

PSC testing has been carried out to simulate industrial rolling processes. This experimental technique can control accurately the deformation conditions, such as temperature, strain rate and strain. In the present paper, FEM was conducted using the commercial general purpose finite

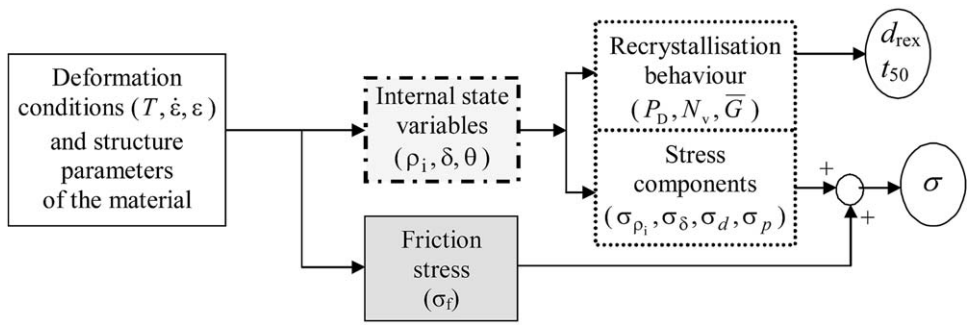

Fig. 1. Schematic drawing of the block diagram of the hybrid model.

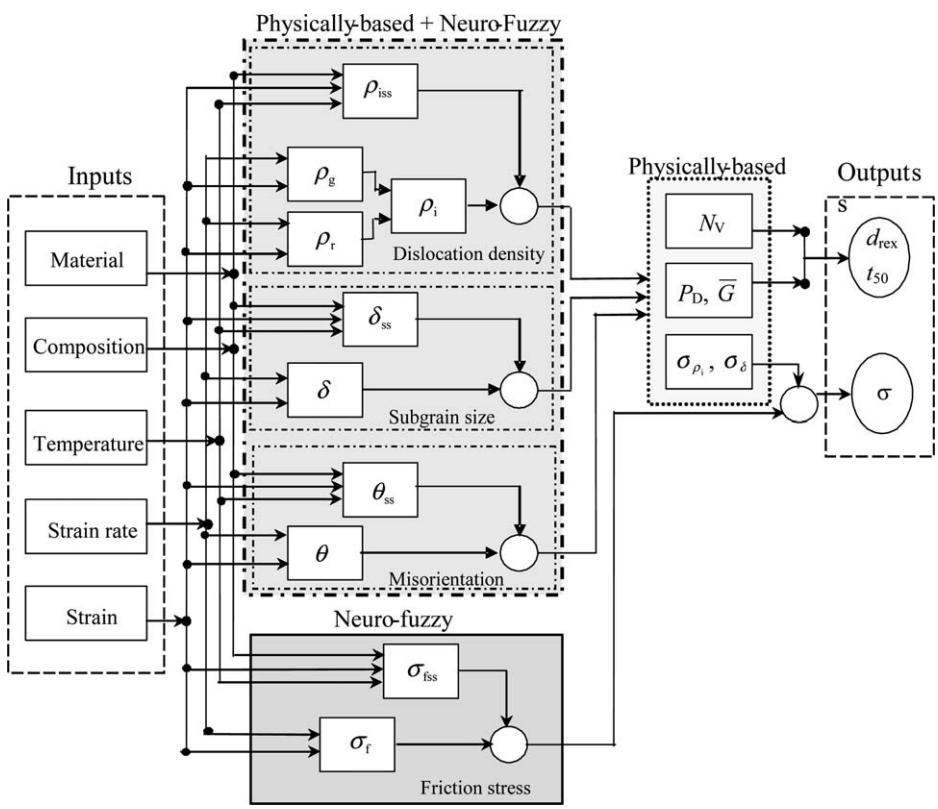

Fig. 2. Schematic drawing of the detailed processes of the hybrid model.

element software MARC to predict distribution of local deformation conditions and flow stress of Al–1% Mg.

The distribution of temperature, strain rate, strain and flow stress in a specimen of dimension 10 mm in thickness and 30 mm in breadth was simulated for deformation by tools of 15 mm in width at a temperature of 400 °C and strain rate of 2/s to 50% reduction. The testing tools are modelled as rigid bodies at a constant temperature of 390 °C. Symmetric conditions were applied at the bottom and one side of the specimen (i.e. 2D), thus only one quarter of the process is modelled. However, for the calculation of deformation load, a 3D

finite element model was also developed to investigate the influence of the material spread in the specimen deformation zone. The model is thermo-mechanically coupled and all the material properties are a function of temperature. The flow stress of the specimen was modelled using both constitutive equations, which are empirical equations derived from experimental data [20], and the developed hybrid model described above, in order to check the applicability of the developed hybrid modelling approach within finite element models.

In the calculations, a heat transfer coefficient of 50 kW/m^2 K at the contact zone was used. The friction algorithm was based on a modified Coulomb law and the surface shear stress τ was calculated by

$$\tau = \mu P_{\mathrm{n}} \frac{2}{\pi} \arctan\left(\frac{v_{\mathrm{r}}}{C_4}\right) \tag{20}$$

where μ is the friction coefficient, C_4 is a constant, v_{r} is the relative velocity and P_{n} is the normal pressure. The basis for the empirical equation used in this calculation can be found in Ref. [20].

5. Results and discussion

The developed hybrid modelling approach has been applied to simulate flow curves, evolution of internal state variables of Al–1% Mg during deformation and subsequent recrystallisation behaviour under constant and transient strain rate conditions. Fig. 3 shows the comparison of the results modelled using the developed hybrid model with experimentally measured data. A generally good agreement between the calculated and measured data has been obtained for all the deformation conditions. This indicates that the hybrid model can be applied successfully to quantitatively describe the evolution of internal state variables and subsequent recrystallisation behaviour for the mentioned deformation and annealing conditions. Comparing the results modelled by physically-based models presented in Ref. [9] and the results modelled by the hybrid model, Fig. 3, shows the latter gives a better fit to experimental data for the internal state variables and subsequent recrystallisation behaviour under transient strain rate conditions.

The prediction of flow curves, evolution of internal state variables for a wide range of deformation conditions and subsequent recrystallisation behaviour has been carried out for different Al–Mg alloys. Fig. 4 shows the predicted results for Al–1% Mg at temperatures of 300, 400 and 500 °C and strain rates of 0.25, 2.5 and 25/s. With increasing temperature and/or decreasing strain rate, the flow stress, internal dislocation density and misorientation across subboundaries decrease, but spacing between subboundaries, recrystallisation time and recrystallised grain size increase for all strain ranges. On the other hand, the flow stress, internal state variables and recrystallisation characteristics change continuously with strain up to steady state for all deformation conditions. In steady state, plastic deformation is accommodated with dynamic balance of increasing dislocations generated by plastic deformation and elimination by the interaction between internal dislocation by an opposite signs and between the moving dislocations and subboundaries [8,9]. In steady state deformation, mean spacing between subboundaries and misorientation across the subboundaries are also saturated, i.e. remain constant with strain [3–9], but recrystallisation time t_{50} and recrystallised grain size d_{rex} decrease continuously with strain at a constant rate. The continuous decrease in recrystallisation time t_{50} and recrystallised grain size d_{rex} arise from the increase in grain boundary area [8,9]. The constant flow stress in steady state indicates that no dynamic recrystallisation occurs in these alloys under the experimental deformation conditions. The strain required to reach steady state conditions increases with decreasing temperature and/or increasing strain rate. All the characteristics of the change in flow stress, internal state variables and recrystallisation behaviour with deformation conditions and strain are as expected from general experimental results [20–22] for other alloys or other deformation conditions. For an Al–5% Mg alloy, similar phenomena to the Al–1% Mg alloy are obtained, but with higher values of flow stress, internal dislocation density and misorientation across subboundaries and smaller values of spacing between subboundaries, recrystallisation time t_{50} and recrystallised grain size than those for Al–1% Mg, as shown in Fig. 5. This arises from the higher

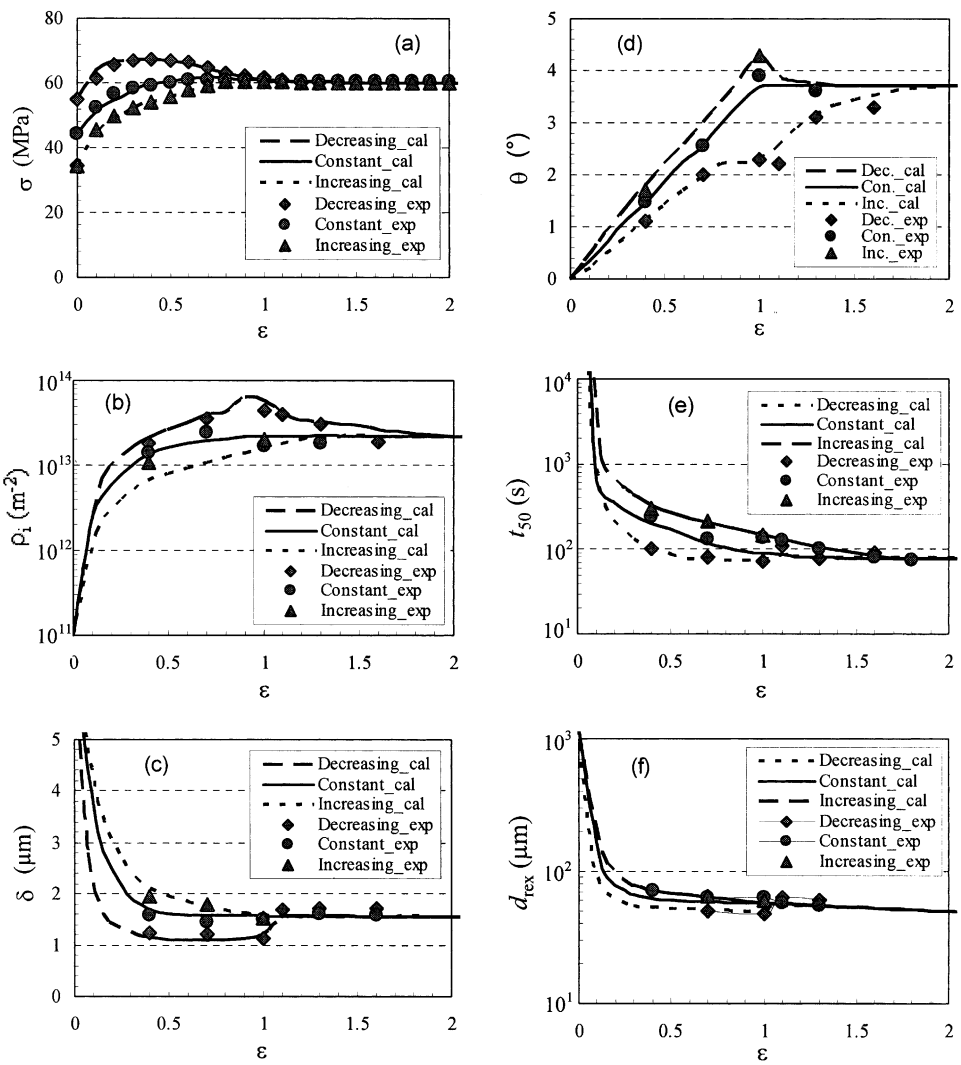

Fig. 3. Comparison of experimental and hybrid-model calculated (a) flow stress, (b) internal dislocation density, (c) subgrain size, (d) misorientation between subgrains, (e) recrystallisation kinetics and (f) recrystallised grain size in Al–1% Mg after PSC deformation at 385 °C and under transient deformation conditions and after annealing at 400 °C (symbols are experimental data and lines are modelled results).

solution hardening due to higher magnesium contents.

The local distribution of deformation conditions such as temperature, strain rate and strain together with the flow stress, which is determined by the internal microstructures within a workpiece during industrial thermomechanical processing is of interest for both scientific research and industrial applications. The developed hybrid model has been embedded into the finite element package by recoding it in Fortran. Fig. 6 shows the load required to deform a specimen of Al–1% Mg at a strain rate of 2/s and temperature of 400 °C in PSC testing calculated by the finite element model in comparison with experimental data. The results can be described as below:

- *Isothermal 2D modelling*: This finite element

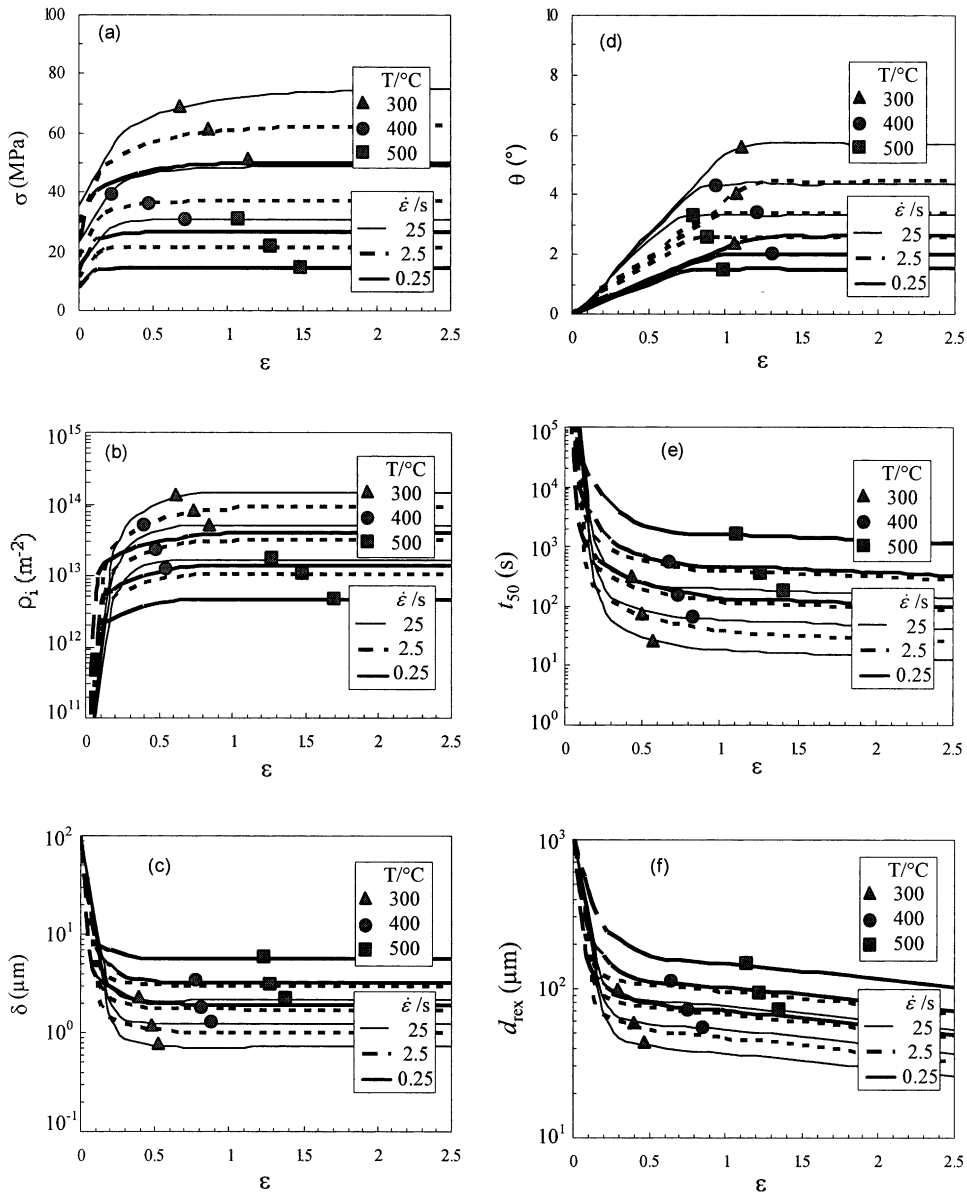

Fig. 4. Evolution of (a) flow stress, (b) internal dislocation density, (c) subgrain size, (d) misorientation between subgrains, (e) kinetics of recrystallisation and (f) recrystallised grain size of Al–1% Mg after annealing at 400 °C calculated by the hybrid model.

model gives an overestimation of the load for all deformation, compared with experimental results. Heat generated by plastic deformation is not included and pure plane strain behaviour has been assumed in this calculation.

- *Coupled 2D modelling*: The heat generated by plastic deformation is included in this calculation. This helps to reduce the load required during the deformation because of the increase in deformation temperature, which was calculated by the equation $T_{\mathrm{def}} = T_{\mathrm{apparent}} + \int \sigma \mathrm{d}\varepsilon / c_{\mathrm{p}}\rho_{\mathrm{D}}$, where T_{apparent} is the setting temperature, c_{p} is the specific heat coefficient and ρ_{D} is the density of the material. When comparing the

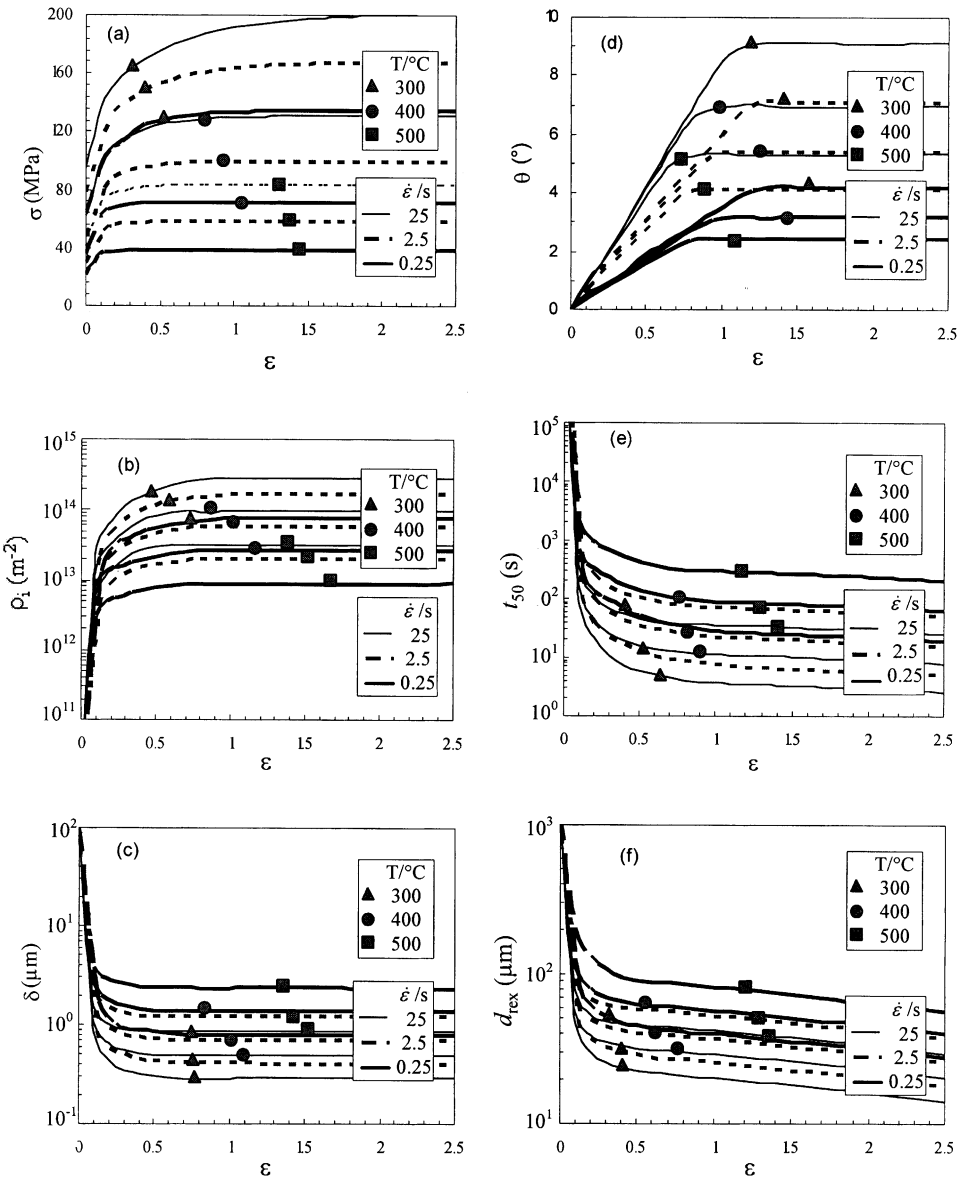

Fig. 5. Evolution of (a) flow stress, (b) internal dislocation density, (c) subgrain size, (d) misorientation between subgrains, (e) kinetics of recrystallisation and (f) recrystallised grain size of Al–5% Mg after annealing at 400 °C calculated by the hybrid model.

calculated results by isothermal and coupled 2D (Fig. 6), the reduction in load increases with increasing deformation (displacement). The calculated load matches experimental data for the deformation after a displacement of 4 mm, but before this displacement the calculated load is still too big compared with experimental data. This can be considered to arise because the relaxation is constrained by the spread. Therefore, the effect of spread on load must be taken into account.

- *Coupled 3D modelling*: This calculation considered the influence of spread of the PSC specimen during plastic deformation by using a 3D

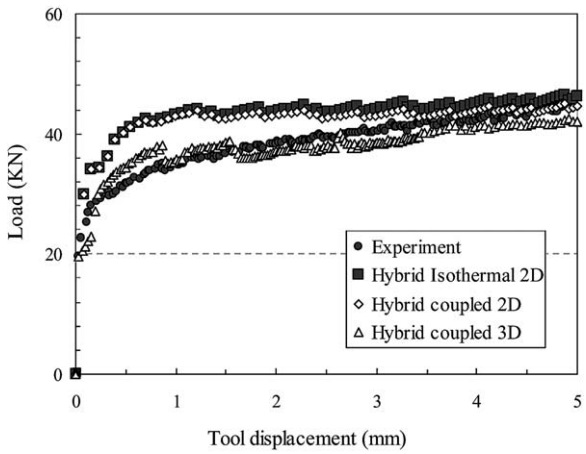

Fig. 6. The load used to deform an Al–1% Mg alloy at 400 °C and 2/s to reduction of 50% in a PSC tests calculated by the finite element model in comparison with experimental data.

modelling approach. The specimen breadth of 30 mm is included in order to account for spread changes. The modelling result shows a much improved fit to the experimental data, indicating that a considerable amount of spread is generated by the PSC testing. A reduction in load arising from the spread of the PSC specimen was observed during this simulation for the initial deformation. As deformation increases, the amount of material to be deformed in the lateral direction of spread, and thus the effect of spread on deformation load, is reduced. This result is in close agreement with the experimental data. The spread of PSC specimens during hot deformation is observed in experimental tests and as a result, 3D modelling is necessary to calculate loads during hot plastic deformation in PSC tests.

The simulation was also carried out using the same sample dimensions and process conditions described in Section 4. The local distribution of deformation conditions such as temperature, equivalent strain rate and equivalent strain were computed by both the empirical equation approach and the developed hybrid model. Based on the simulated local distribution of deformation conditions, the local distribution of equivalent flow stress was calculated. Generally, a good agreement between the local distribution of all the deformation condition parameters and the flow stress modelled by the empirical and the developed hybrid models was obtained, Fig. 7. Note that the slight discrepancies in the contours arise from the nature of both models. The good agreement between modelled results by the FEM using the empirical and the developed hybrid model shows that the hybrid modelling approach can be applied as successfully as empirical equations within FEM code, which is essential to predict mechanical behaviour under conditions close to those for real industrial thermomechanical processing conditions as explained in details in Refs. [16,23,24]. The current setting of the system is based on a 1.1 GHz Pentium III machine running Windows XP operating system. The calculation time is roughly 3 h for 2D model (5 h for the 3D model) using the hybrid model, compared with 1 h for the 2D model (3 h for the 3D model) calculation time using the empirical approach. The calculation time is three times longer for the 2D model (about two times for the 3D model) using the hybrid model than empirical approach, but with the significant improvement of computer processing speed, this will not be the key parameter in the simulation environment. The big advantage of using the hybrid modelling approach is, however, as mentioned above, that it is based on physical principles and can be extrapolated into much wider processing conditions.

6. Conclusions

- The developed hybrid modelling approach combining physically-based models and neuro-fuzzy models has been successfully applied to quantitatively describe flow stress and evolution of internal state variables during hot deformation under constant and transient conditions and recrystallisation behaviour during subsequent annealing of Al–1% Mg.
- The hybrid modelling approach can be used successfully to predict flow stress and the evolution of internal state variable during hot deformation under different conditions and subsequent recrystallisation behaviour for different Al–Mg alloys.

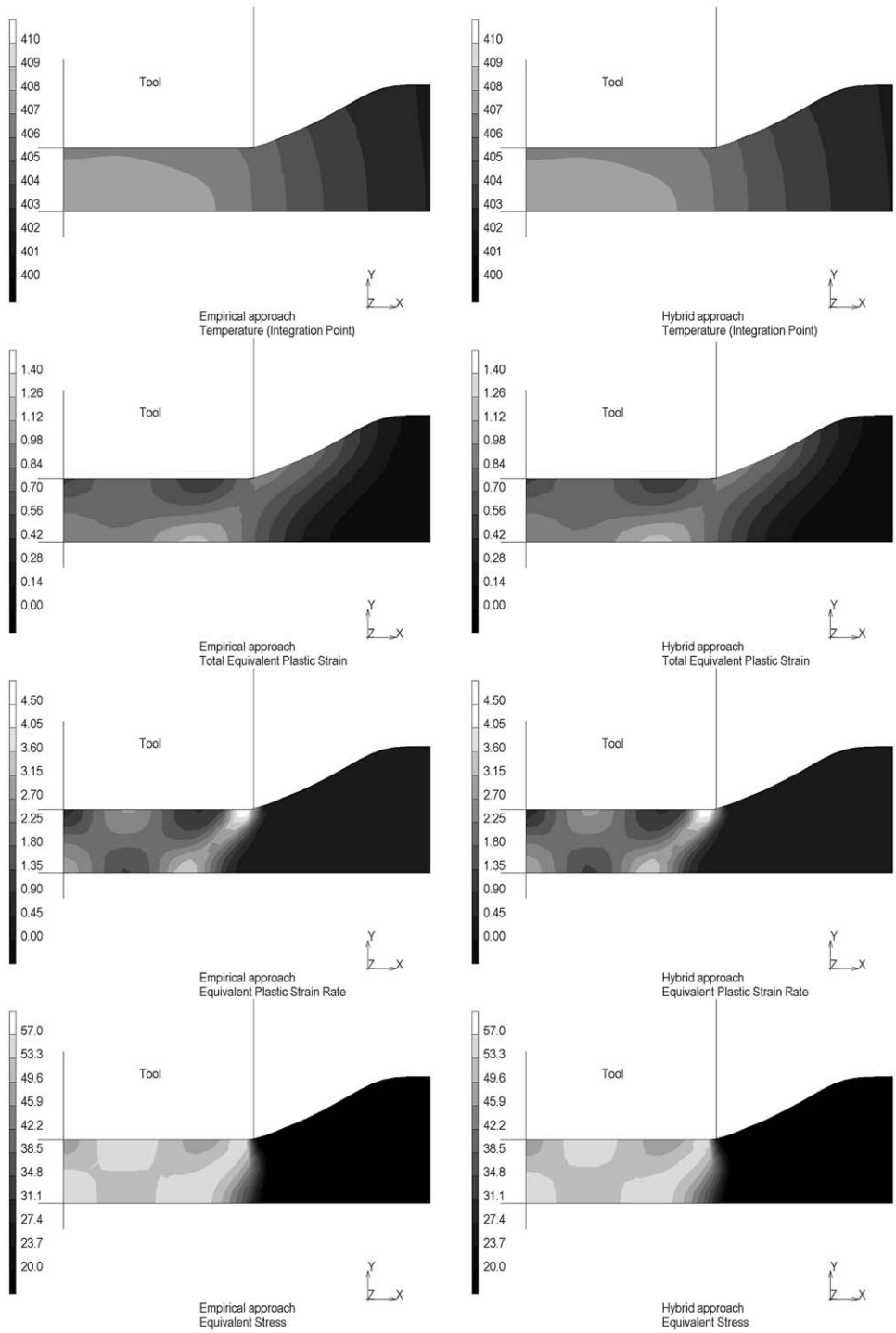

Fig. 7. Comparison of the distribution of temperature, strain rate, strain and flow stress calculated by finite element model using empirical constitutive equations (left) and the developed hybrid modelling approach (right).

- Comparison of the local distributions of deformation conditions and flow stress within a PSC test specimen simulated by FEM using the empirical equations and the developed hybrid model shows a very similar result, indicating that the hybrid modelling approach can be applied within FEM code. The physically-based components in the hybrid model facilitate extrapolation beyond process conditions utilised for the block-box components, and this is essential to predict microstructural and mechanical behaviour close to those for real industrial thermomechanical processing conditions.

Acknowledgements

The authors are grateful to the UK Engineering and Physical Sciences Research Council for financial support with grant number GR/L 50198.

References

[1] Beynon JH, Ingham P, Teichert H, Waterson K, editors. Proceedings of the Second International Conference on Modelling of Metal Rolling Processes. London: The Institute of Materials; 1996.
[2] Beynon JH, Clark MT, Ingham P, Kern P, Waterson K, editors. Proceedings of the Third International Conference on Modelling of Metal Rolling Processes. London: The Institute of Materials; 1999.
[3] Nix WD, Ilschner B. In: Haasen P, Gerold V, Kostorz G, editors. Proceedings of the Fifth International Conference on the Strength of Metals and Alloys (ICSMA 5). Oxford: Pergamon Press; 1980. p. 1503.
[4] Blum W. In: Mughrabi H, editor. Plastic deformation and fracture of materials. Cahn RW, Haasen P, Kramer EJ editors. Materials science and technology, 6. Weinheim: VHC Publication; 1993. p. 359.
[5] Zhu Q, Blum W. In: Hosoi Y, Yoshinaga H, Oikawa H, Maruyama K, editors. Proceedings of Aspect of High Temperature Deformation and Fracture in Crystalline Materials. Sendai 980, Japan: The Japan Institute of Metals; 1993. p. 649.
[6] Nes E. Prog Mater Sci 1997;41:129.
[7] Zhu Q, Sellars CM. In: Beynon JH, Ingham P, Teichert H, Waterson K, editors. Proceedings of the Second International Conference on Modelling of Metal Rolling Processes. London: The Institute of Materials; 1996. p. 158.
[8] Zhu Q, Shercliff HR, Sellars CM. In: Chandra T, Sakai T, editors. Proceedings of the International Conference on Thermomechanical Processing of Steels and Other Materials (THERMEC'97). Wollongong/Australia: TMS; 1997. p. 2039.
[9] Sellars CM, Zhu Q. Mater Sci Eng 2000;A280:1.
[10] Sellars CM, Zhu Q. In: Bieler TR, Lalli LA, MacEwen SR, editors. Proceedings of the Symposium on Hot Deformation of Aluminium Alloys II, Rosemont II. Warrendale, PA, USA: The Minerals, Metals and Materials Society; 1998. p. 185.
[11] Löffler HU, Gade D, Döll R, Muller H, Peuker T, Sorgel G. In: Proceedings of IFAC Workshop, Future Trends in Automation in Mineral and Metal Processing, Finland, 22–24 August. 2000. p. 410.
[12] Abbod MF, Talamantes-Silva J, Zhu Q, Linkens DA. In: de Silva CW, Karray F, editors. Proceedings of the 2002 IEEE International Symposium on Intelligent Control (ISIC2002), Vancouver, British Columbia, Canada, 27–30 October. Omnipress: IEEE Control Systems Society; 2002. p. 321–6.
[13] Abbod MF, Linkens DA, Zhu Q. Mater Sci Technol 2002;A333:397.
[14] Zhu Q, Abbod MF, Sellars CM, Linkens DA. In: Lewis T, editor. Proceedings of International Conference of Metallurgists. Montreal, Canada: Canadian Inst of Mining, Metallurgy and Petroleum; 2002. p. 701.
[15] Talamantes-Silva J, Beynon JH. Hot rolling simulation of long products using finite element modelling. In: Beynon JH, Clark MT, Ingham P, Kern P, Waterson K, editors. Metal rolling processes 3. London, UK: IOM Communications Ltd; 1999. p. 160–8.
[16] Auzinger D, Humber G, Luger A. Full metallurgical control of the mechanical properties of hot rolled strip—a summary of more than 2 years of experimental experience. In: Palmiere Eric J, Mahfouf M, Pinna C, editors. Thermomechanical processing: mechanics, microstructure and control. Sheffield, UK: BBR Publications Ltd, in press.
[17] McLaren A, Sellars CM. Mater Sci Technol 1992;8:1090.
[18] Linkens DA, Kandiah S. Trans IChemE 1996;74:77.
[19] Higashi M, Klir GJ. IEEE Trans Syst, Mon and Cybernetics 1984;14:349.
[20] Shi H, McLaren AJ, Sellars CM, Shahani R, Bolingbroke R. Mater Sci Technol 1997;13:210.
[21] McQueen HJ, Blum W, Zhu Q, Demuth V. In: Bieler TR, Jonas JJ, editors. Proceedings of the International Symposium on Advances in Hot Deformation and Texture. Warrendale, PA: TMS-AIME; 1994. p. 235.
[22] Yavari P, Langdon TG. Acta Metall 1982;30:2181.
[23] Mirza MS, Sellars CM. Mater Sci Technol 2001;17:1133.
[24] Mirza MS, Sellars CM. Mater Sci Technol 2001;17:1142.